Supplementary Figure 1

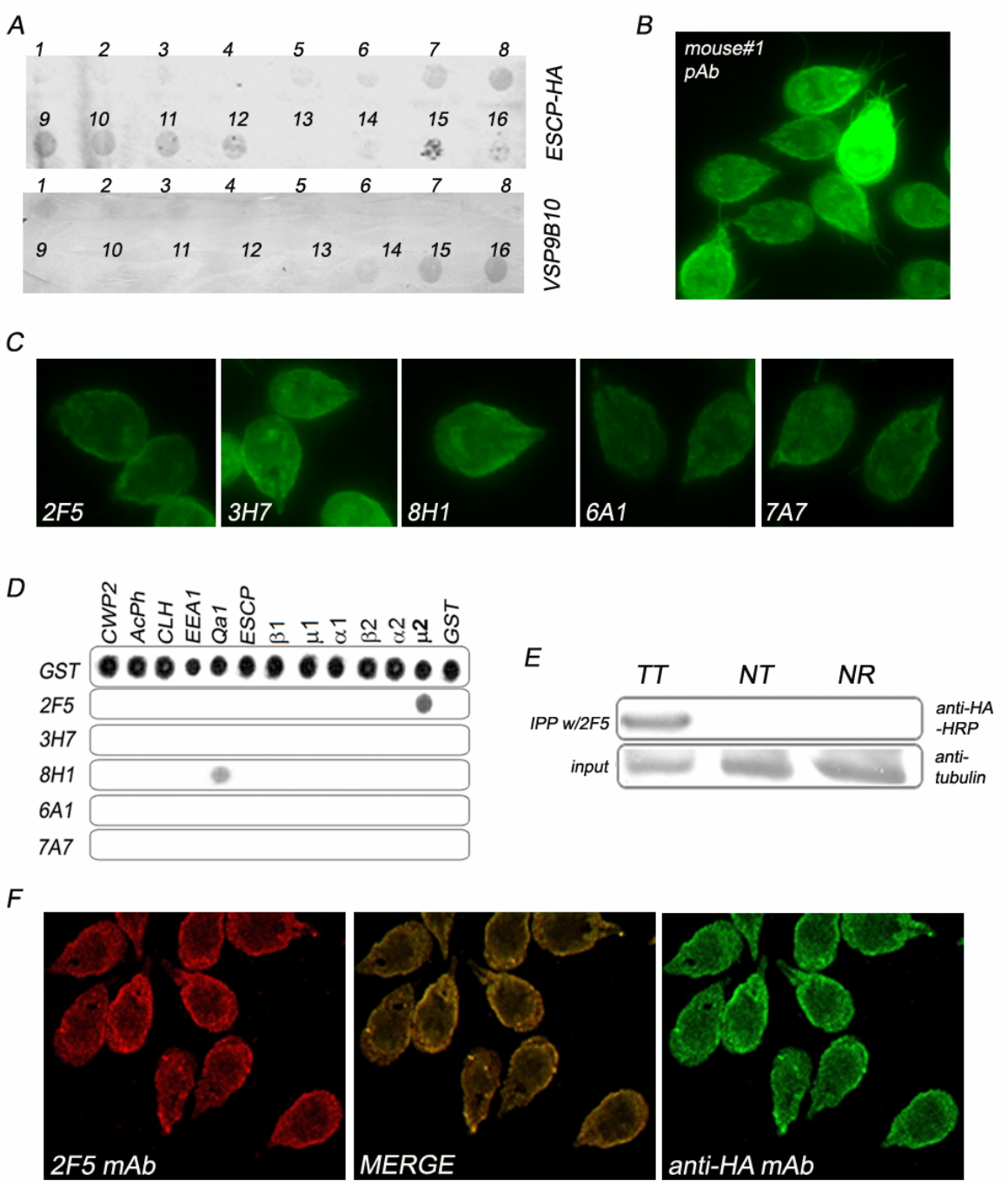

S1. (A) Dot-blotting of ESCP transgenic trophozoites fractionated on sucrose gradients. Fractions were collected from the top (fraction 1) to the bottom (fraction 16) and analyzed for ESCP (PVs) and VSP9B10 (plasma membrane) localization. (B) The PV immunized mouse #1 serum detects proteins located in the PVs and surface after immunization in IFA and epifluorescence microscopy. (C) After fusion, the hybridomas 2F5, 3H7, 8H1, 6A1, and 7A7 identified proteins that might be located in the PVs. (D) Dot-blotting of GST-tagged acid phosphatase (AcPh), clathrin heavy chain (CLH), Early Endosome Antigen 1 (EEA1), SNARE (Qa1), encystation-specific cysteine protease (ESCP), and the subunits of AP1 (β1, μ1, α1) and AP2 (β2, μ2, α2) shows that 2F5 and 8H1 mAbs recognized *Giardia* μ2 and Qa1, respectively. GST-Cyst wall protein 2 (CWP2) and GST alone were used as negative controls. (E) Immunoprecipitation assay shows that 2F5 mAb is able to recognize the fusion protein, HAμ2. Immunoblotting was revealed with HRP-conjugated anti-HA mAb, and anti-tubulin was detected on the same membrane as a loading control (bottom panel). TT: HAμ2-transfected trophozoites. NT: control assay using non-transfected trophozoites. NR: control assay using the non-related 7D2 mAb. (F) Colocalization of gμ2 and HAμ2 in the PVs using the mAbs 2F5 and anti-HA.

Supplementary Figure 2

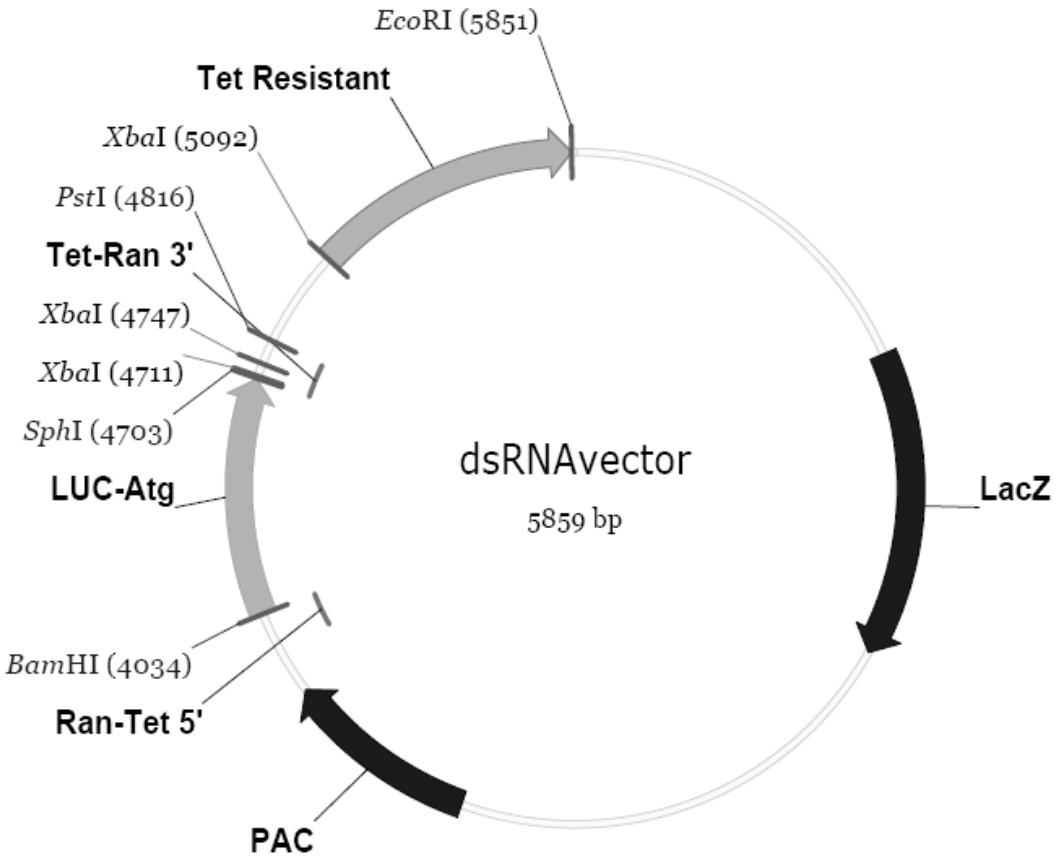

Ran-Tet 5′

```
CGCTAGCAAG ATCTAAAATA AATTAAATCG AAATTAAAAC TTTAAGATCT
GCGATCGTTC TAGATTTTAT TTAATTTAGC TTTAATTTTG AAATTCTAGA

CCTAGTCCCT ATCAGTGATA GAGACTAGTC CCTATCAGTG ATAGAGACTA
GGATCAGGGA TAGTCACTAT CTCTGATCAG GGATAGTCAC TATCTCTGAT
```

Ran-Tet 3′

```
TAGTCTCTAT CACTGATAGG GACTAGTCTC TATCACTGAT AGGGACTAGG
ATCAGAGATA GTGACTATCC CTGATCAGAG ATAGTGACTA TCCCTGATCC

AGATCTTAAA GTTTTAATTT CGATTTAATT TATTTTAGAT CTTGCTAGCG
TCTAGAATTT CAAAATTAAA GCTAAATTAA ATAAAATCTA GAACGATCGC
```

S2: pdsRNA Tet-inducible vector. This vector was developed for inducible expression of double-stranded RNAs in *Giardia*. It contains opposing *Giardia ran* promoters (in grey) with tetracycline (Tet) operator elements (underlined) and is designed for insertion and double-stranded expression of PCR products. It also has a puromycin cassette under the control of an endogenous, non-regulated *gdh* promoter. The gμ2 targeting sequence was amplified by PCR from genomic *Giardia* DNA and introduced between opposing tetracycline-inducible *Giardia ran* promoters.

Supplementary Figure 3:

A

```
Hs-μ2       1 MIGGLFIYNHKGEVLISRVYRDDIGRNAVDAFRVNVIHARQQVRSPVTNIARTSFFHVKR
Rn-μ2       1 MIGGLFIYNHKGEVLISRVYRDDIGRNAVDAFRVNVIHARQQVRSPVTNIARTSFFHVKR
Gi-μ2       1 MIKAVILLDDVGELILQRVFMGSFDKTALDLLRTHVLGG--SISQPILRIPPHIYAYKRC

Hs-μ2      61 SNIWLAAVTKQNVNAAMVFEFLYKMCDVMAAYFG-KISEENIKNNFVLIYELLDEILDFG
Rn-μ2      61 SNIWLAAVTKQNVNAAMVFEFLYKMCDVMAAYFG-KISEENIKNNFVLIYELLDEILDFG
Gi-μ2      59 DALHFFCTISAKTDTMSAITFLDRFYKAMGAFLKEKELAGNLRKFIPLIHELLDEMIDNG

Hs-μ2     120 YPQNSETGALKTFITQQGIKSQHQTKEEQSQITSQVTGQIGWRREGIKYRRNELFLDVLE
Rn-μ2     120 YPQNSETGALKTFITQQGIKSQHQTKEEQSQITSQVTGQIGWRREGIKYRRNELFLDVLE
Gi-μ2     119 DVQTTDPEVLKLFIQTR--QKINKAEESNQQITVQATGALSHRRQGIIYKRNEIFIDVVE
                                                          *

Hs-μ2     180 SVNLLMSPQGQVLSAHVSGRVVMKSYLSGMPECKFGMNDKIVIEKQG---KGTADETSKS
Rn-μ2     180 SVNLLMSPQGQVLSAHVSGRVVMKSYLSGMPECKFGMNDKIVIEKQG---KGTADETSKS
Gi-μ2     177 SVNAMFNNVGQSLHADVSGKIIIKNSLTGMPDCSFGFNDRVVGAGANGPRTEVAQQVAGV

Hs-μ2     237 GKQSIAIDDCTFHQCVRLSKFDSERSISFIPPDGEFELMRYRTTKDIILPFRVIPLVREV
Rn-μ2     237 GKQSIAIDDCTFHQCVRLSKFDSERSISFIPPDGEFELMRYRTTKDIILPFRVIPLVREV
Gi-μ2     237 SQAGVVMDDLSFHHCVRLGNFAVDRSIAFVPPDGEFQLMAFRVTEEVKEPFSIKPIVTVH

Hs-μ2     297 GRTKLEVKVVIKSNFKPSLLAQKIEVRIPTPLNTSGVQVICMKGKAKYKASENAIVWKIK
Rn-μ2     297 GRTKLEVKVVIKSNFKPSLLAQKIEVRIPTPLNTSGVQVICMKGKAKYKASENAIVWKIK
Gi-μ2     297 GRNRMEIVLNLRCGIPSNNVAEHVIVSVPMPSNVSDVTAIESLGKCRLRKDGQAAEWRIK

Hs-μ2     357 RMAGMKESQISAEIELLPTN--DKKKWARPPISMNFEVPFAPS-GLKVRYLKVFEPKLNY
Rn-μ2     357 RMAGMKESQISAEIELLPTN--DKKKWARPPISMNFEVPFAPS-GLKVRYLKVFEPKLNY
Gi-μ2     357 SITGGTTATLSMEVQCVSSSIDLREWRRPPLAMNFDIPMYTASGIEVRYIRIIAQEG--

Hs-μ2     414 SDHDVIKWVRYIGRSGIYETRC
Rn-μ2     414 SDHDVIKWVRYIGRSGIYETRC
Gi-μ2     415 --YETEKWLTYKTSAGTYQIRW
                   *
```

B

No	Hit	Prob	E-value	P-value	Score	SS	Cols	Query HMM	Template HMM
1	2vgl_M AP-2 complex subunit *Rattus novergicus*	100.0	0	0	756.6	52.2	426	1-433	1-434 (435)
2	1w63_M Adaptor-related protein *Mus musculus*	100.0	0	0	740.4	42.7	416	2-433	3-421 (423)
3	1i31_A Mu2 Adaptin Subunit Complexed with Egfr Internalization Peptide *Rattus novergicus*	100.0	0	0	563.7	31.9	307	121-433	1-313 (314)
4	2hf6_A Coatomer subunit *Homo sapiens*	100.0	5.2E-28	2.4E-32	209.6	15.7	135	1-135	12-149 (149)

S3: A) 2D gμ2 subunit alignment. *Homo sapiens* μ2 (Hs-μ2), *Rattus norvegicus* μ2 (Rm-μ2), and *Giardia* μ2 (Gi-μ2) protein sequences are compared using ClustalW Multiple Sequence Alignment. Consensus is shown in red. The conserved residues, D173 and W420, involved in μ2 binding are denoted by asterisks (*). **B) 3D gμ2 subunit prediction.** *Giardia* μ2 (gμ2) protein sequence was used for sequence database searching and structure prediction by the hidden Markov models (HMMs) (Söding J.; 2005). The E-value <1 and the probabilities of 100.0 indicate a true positive of the gμ2 3D structure predicted from *Rattus norvegicus* μ2, Mus musculus μ2, and *Homo sapiens* μ2.

Supplementary Figure 4

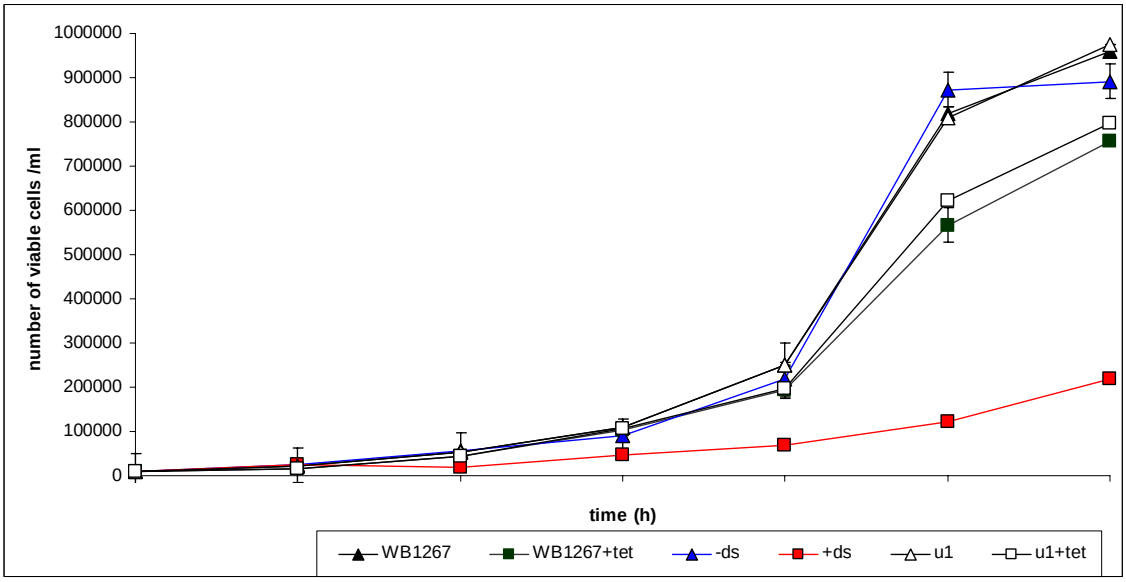

S4. Depletion of gμ2 reduces trophozoite growth. Growth of *Giardia lamblia* WB1267 wild-type (WB1267), gμ1-depleted, and gμ2-depleted (+ds) trophozoites. At time 0, 10^4 trophozoites were inoculated to growth medium and trophozoite numbers were determined every 12 h over a period of 3 days. The growth of +ds trophozoites is dramatically reduced compared with -ds. Tet addition to wild-type or gμ1-depleted cells showed a minor effect on growth (WB1267+tet, μ1+tet) compared to cultures without Tet. Data represent the mean ± s.d. for n=6 in four independent experiments.

Supplementary Figure 5

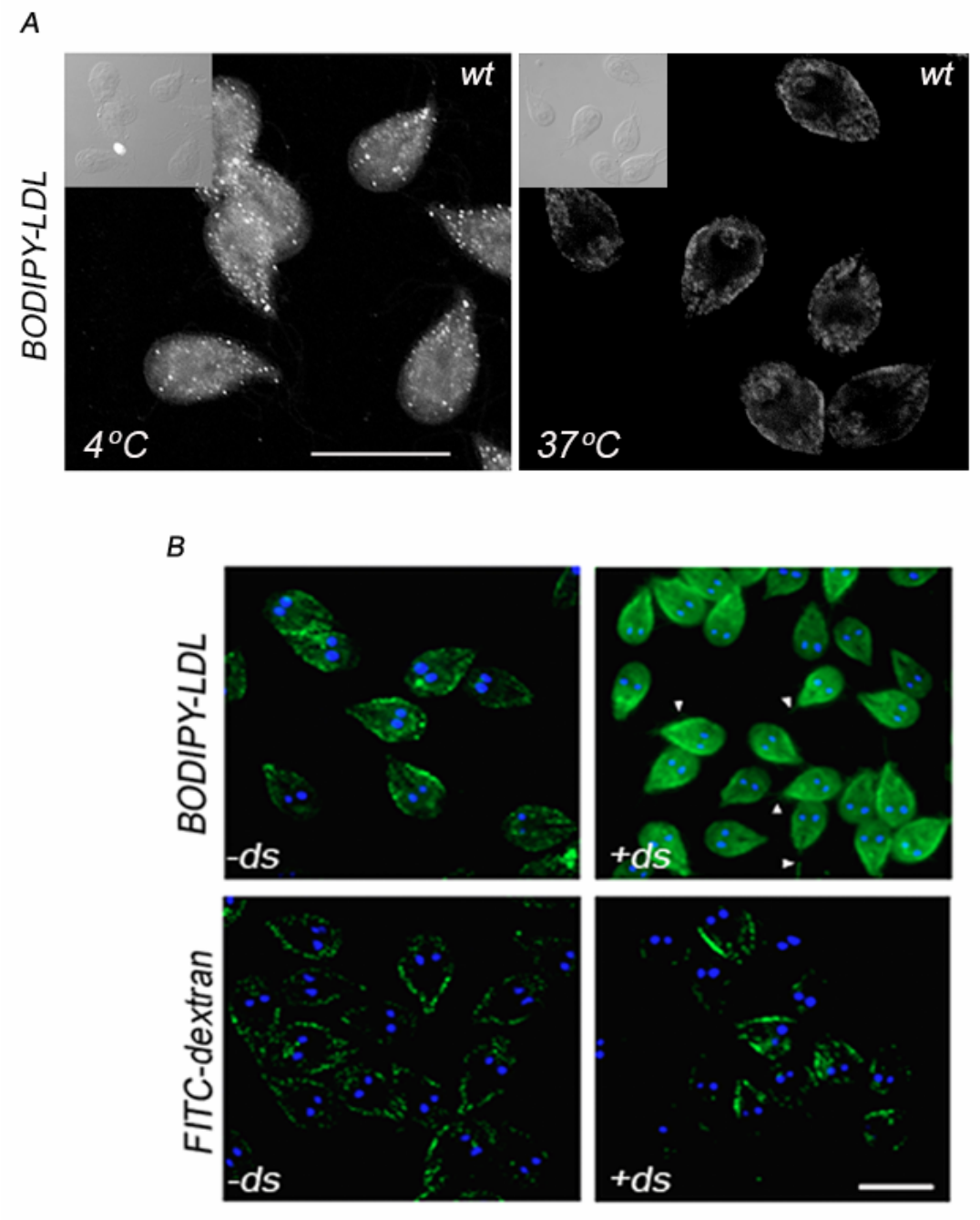

S5. LDL binds to a specific protein on the surface of the trophozoite. (A) Epifluorescence microscopy of BODIPY-LDL at 4°C (endocytosis is inhibited) shows that the LDL remains on the surface, probably bound to a membrane receptor (4°C), and is then internalized when the same cells are returned to 37°C for 2 h (37°C). Bar, 10 µm. wt: wild-type *Giardia* trophozoites. Contrast phase images are shown in the inserts. (B) Epifluorescence microscopy of uptake assays using fluorophore-labelled LDL (BODIPY-LDL) and dextran (FITC-dextran) shows that both the LDL and dextran localize to the PVs in non-permeabilized trophozoites (left panels, -ds). When gµ2 is depleted, the LDL remains on the surface, including the flagella (arrowheads), while dextran is still internalized to the PVs (right panels, +ds). Bar, 10 µm

Supplementary Figure 6

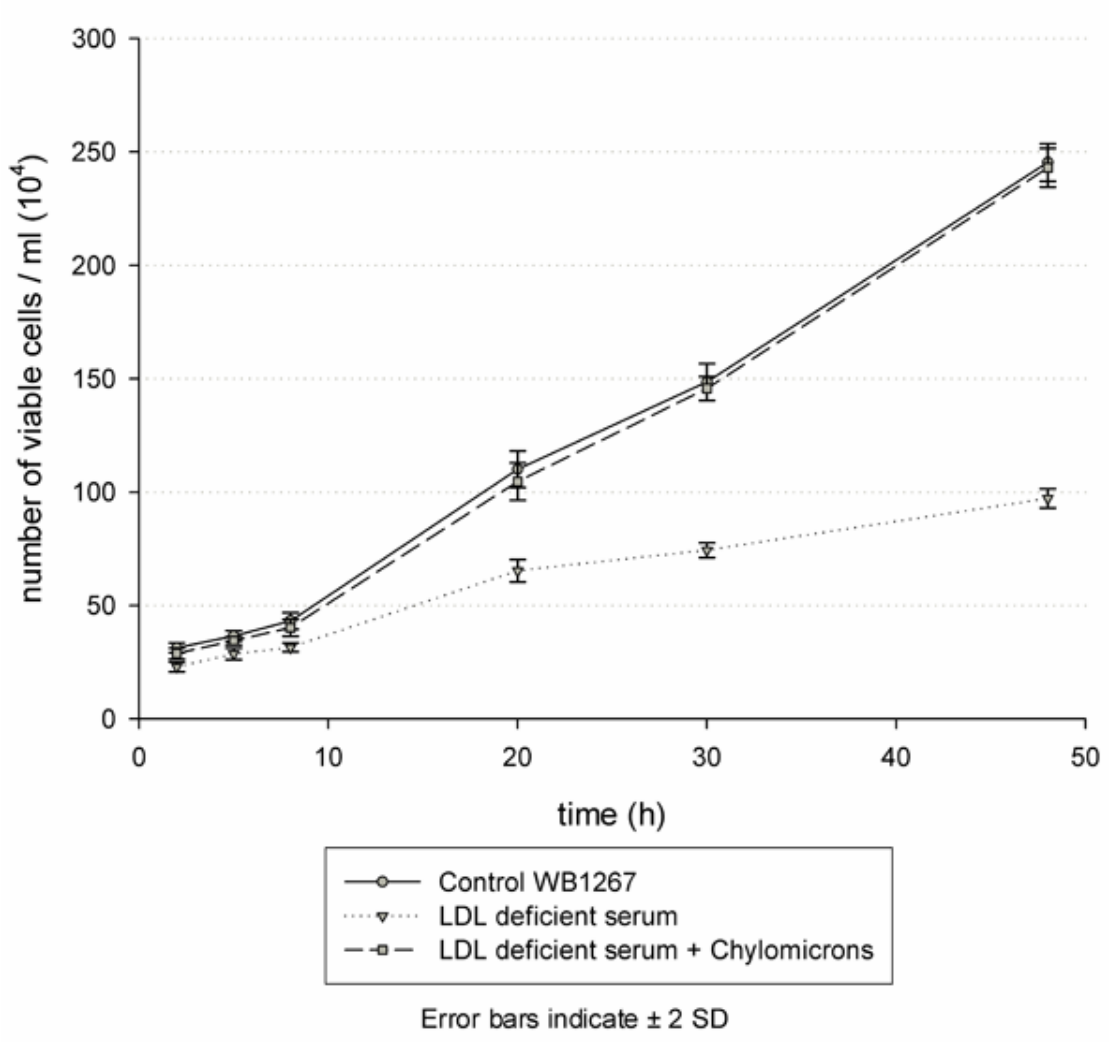

S6. Addition of chylomicrons restores trophozoite growth. Growth curve of trophozoites grown in medium lacking LDL (lipoprotein-deficient serum) shows a reduction in growth of about 40% at 20 h and 60% at 48 h, compared with trophozoites grown in medium containing LDL (control WB1267). Growth curve of trophozoites grown in lipoprotein-deficient medium shows cell recovery with the addition of chylomicrons (lipoprotein-deficient serum + Chylomicrons). Repeated measures ANOVA: $F=2244.1$; $df=2$; $p<0.001$. Error bars indicate ± 2SD.